Original Article

Sexual Development

Sex Dev 2007;1:42–58
DOI: 10.1159/000096238

Received: July 17, 2006
Accepted after revision: August 21, 2006

mRNA Expression Analysis and the Molecular Basis of Neonatal Testis Defects in *Dmrt1* Mutant Mice

U. Fahrioglu M.W. Murphy D. Zarkower V.J. Bardwell

Department of Genetics, Cell Biology, and Development, University of Minnesota, Minneapolis, Minn., USA

Key Words
DM domain · *Dmrt1* · Gdnf · Gonocyte · Sertoli · Sexual differentiation · *Stella* · Testis

Abstract
Transcriptional regulators containing the DM domain DNA binding motif have been found to control sexual differentiation in a diverse group of metazoan animals including vertebrates, insects, and nematodes, suggesting that these proteins may comprise a very ancient group of sexual regulators. *Dmrt1*, 1 of 7 mammalian DM domain genes, is essential for several aspects of testicular differentiation in mice. The *Dmrt1* mutant phenotype becomes apparent shortly after birth, and culminates in severe testicular dysgenesis. To better understand the roles of *Dmrt1* in testicular development we have performed a more detailed analysis of its mutant phenotypes, and we have used mRNA expression profiling to identify genes misregulated in the neonatal *Dmrt1* mutant testis. We find that *Dmrt1* mutant germ cells fail to undergo several of the normal postnatal events of germ cell development, including radial movement, mitotic proliferation, differentiation into spermatogonia, and initiation of meiosis, and they die by P14. During this period *Dmrt1* mutant Sertoli cells fail to polarize and form tight junctions, and fail to cease proliferation, eventually filling the seminiferous tubules. Expression profiling at P1 and P2 in *Dmrt1* mutant testes indicates defects in several important testicular signaling pathways (Gdnf, retinoic acid, TGFβ, FSH), and detects elevated expression of the pluripotency marker *Stella/Dppa3/Pgc7*, providing insight into the molecular basis of *Dmrt1* testis defects. This work also identifies a number of new candidate testicular regulators for further investigation.

Gonadal development in mammals is initiated during embryogenesis and culminates after puberty in each sex with the formation of fully differentiated organs dedicated to the production of gametes and sex hormones. In the mouse, gonadal development begins around 9.5 days post-coitus (E9.5) when the urogenital ridge or bipotential gonad forms from a thickening of the coelomic epithelium and then is colonized by primordial germ cells (PGCs) that migrate from the dorsal mesentery (for a recent review of embryonic gonadogenesis, see Brennan and Capel, 2004). Shortly after the bipotential gonad is formed, sex determination and sexual differentiation begin, with *Sry* expression detectable by about E10.5 and the first morphological differences between testis and ovary apparent by about E12.0. During embryogenesis germ cell and somatic cell sex is determined, the primary somatic cell types are specified, and the basic anatomy of

This work was funded by the NIH (GM059152).

KARGER

Fax +41 61 306 12 34
E-Mail karger@karger.ch
www.karger.com

1661–5425/07/0011–0042$23.50/0

Accessible online at:
www.karger.com/sxd

Vivian J. Bardwell
Department of Genetics, Cell Biology, and Development, University of Minnesota
6–160 Jackson Hall, 321 Church St.
Minneapolis, MN 55455 (USA)
Tel. +1 612 626 7028, Fax +1 612 626 7031, E-Mail bardw001@umn.edu

the gonad is established by morphological changes including the formation of testis cords in the male gonad and follicles in the female gonad.

The basic gonad formed in the embryo further differentiates postnatally in preparation for gametogenesis. In males, the events of the first postnatal week include a radial migration of gonocytes from the central position in the seminiferous tubule that they occupy in the embryo outward to the periphery (Nagano et al., 2000). In this position they can make close contact with the surrounding basement membrane and with neighboring Sertoli cells, and they form a stem cell population capable of supporting sustained gametogenesis. During this period the gonocytes also undergo a brief period of mitotic proliferation and differentiate into spermatogonia, which begin to produce meiotic cells, starting in the first few postnatal days (Ogawa et al., 2005). During early postnatal development Sertoli cells begin to differentiate into mature polarized cells whose basal surface is in close apposition with the basement membrane surrounding each tubule (Mruk and Cheng, 2004). The mature Sertoli cells also form a network of tight junctions comprising the blood/testis barrier.

Substantial progress has been made in recent years identifying genes required for each step of gonadal development, including formation of the bipotential gonad, sex determination, differentiation and signaling between cell types, and some aspects of postnatal differentiation (Brennan and Capel, 2004). Among these events, comparatively little is known regarding the genetic control of early postnatal testis differentiation. As described above, this period is critical for testis development, as it is the time during which the germ line stem cell population is established, supporting cells are positioned and differentiated, and the stage is set for sustained sperm production.

One gene required for early postnatal testis development is *Dmrt1*, which encodes a protein with a DM domain, a DNA binding motif first identified in the *Drosophila* sexual regulator *Doublesex* and the *C. elegans* sexual regulator MAB-3 (Erdman and Burtis, 1993; Raymond et al., 1998). In general, regulators of sexual differentiation have been poorly conserved between distantly related groups of animals, but the DM domain family proteins are an apparent exception. DSX and MAB-3 not only share a structurally unique DNA binding motif (Raymond et al., 1998; Zhu et al., 2000) but also control multiple aspects of sexual differentiation (Baker and Ridge, 1980; Shen and Hodgkin, 1988). Because some of their functions are analogous, it appears likely that these genes arose from more ancient DM domain sexual regulators (Yi and Zarkower, 1999; Zarkower, 2001; Hodgkin, 2002).

Dmrt1 appears likely to regulate sexual differentiation in most or perhaps all vertebrates. In humans, *DMRT1* is expressed only in the testis and maps to 9p24.3 (Raymond et al., 1998, 1999b), within a region deleted in patients with XY gonadal dysgenesis (Crocker et al., 1988; Ogata et al., 1997; Ion et al., 1998). In birds, which have ZZ/ZW sex determination, *DMRT1* is Z-linked (Nanda et al., 1999), is expressed at higher levels in ZZ than ZW genital ridges during and after sex determination (Raymond et al., 1999a; Smith et al., 1999), and may be subject to regulation by a sex-specific non-coding RNA (Teranishi et al., 2001). In reptiles with temperature-dependent sex determination, *Dmrt1* mRNA expression has been shown to be elevated at the time of sex determination in genital ridges from embryos incubated at male-promoting temperatures (Smith et al., 1999; Kettlewell et al., 2000). Similarly, *Dmrt1* is expressed early and male-specifically in the developing gonads of a variety of fish species (e.g., Marchand et al., 2000).

Correlative studies such as those just described strongly suggest a widespread role for *Dmrt1* homologs in vertebrate sex determination and/or gonadal differentiation. Functional data exist only in two species, a mammal and a fish, but confirm the importance of *Dmrt1* in the testicular development. In the mouse, mutation of *Dmrt1* severely disrupts postnatal testis differentiation (Raymond et al., 2000). In the medaka fish, a recent duplication of *Dmrt1* gave rise to the *DMY*/*Dmrt1bY* gene (Nanda et al., 2002; Volff et al., 2003). The chromosome containing this gene serves as a neo-Y chromosome, and spontaneous mutations in the gene result in male-to-female sex reversal (Matsuda et al., 2002). From the available data, it is clear that Dmrt1 is a critical regulator of testis development whose involvement in male gonad development predates the rise of the vertebrates and has been retained as new sex-determining mechanisms have arisen.

We showed previously that *Dmrt1* null mutant mice have defects in postnatal testis differentiation including failure of radial gonocyte movement, death of germ cells, and abnormal Sertoli cell differentiation and proliferation, and that the mutant testes ultimately undergo severe degeneration of cord structure and cellular organization (Raymond et al., 2000). To gain insight into the molecular basis of the *Dmrt1* mutant phenotype, we have performed a more detailed analysis of the early postnatal defects in *Dmrt1* mutant testes in tandem with expression profiling comparing mRNAs in wild type versus *Dmrt1* mutant

Table 1. Primers for real-time RT-PCR

Gene name	Sequence	T_m	Direction	Pair product length	Primer number
Cidea	CAAGCAACCAAAGAAATCGGG	56.1	F	188 bp	VBp 788
	CAGCATAGGACATAAACCTCAGCAG	56.2	R		VBp 789
Occludin	TGATGAACAGCCCCCCAATG	57.7	F	101 bp	VBp 792
	TGTCAACTCTTTCCGCATAGTCAG	55.2	R		VBp 793
Cf-i	ATTTCCCAACGAGTCTGTCCTTC	55.2	F	193 bp	VBp 796
	CAGTCCACCTCACCATTACACTTG	55.1	R		VBp 797
Stella	TTGTTGTCGGTGCTGAAAGACC	56.5	F	116 bp	VBp 798
	CATCTGAATGGCTCACTGTCCC	55.8	R		VBp 799
Dmrt1	TGGCAGATGAAGACCTCAGAGAG	55	F	159 bp	VBp 802
	CGAGAACACACTGGCTTTGGC	57.1	R		VBp 803
Testatin	GAACACATTCAACCAGGAAAGTCAG	55.8	F	217 bp	VBp 805
	ACCGACAGTAAACAGGCAGGTG	55.6	R		VBp 806
Nkx3.1	GGACCCACCAAGTATCCGGCATAG	67.6	F	136 bp	VBp 807
	TGCTTGGTGACCTGGGGGGCACTT	67.9	R		VBp 808
FSHR	TTCCTCTGCCAAGATAGCAAGG	66	F	133 bp	VBp 826
	TTCTCCAGGTCCCCAAATCC	62	R		VBp 827

testes. Expression profiling at P1 and P2 identifies 56 mRNAs with elevated expression and 37 with reduced expression in the *Dmrt1* mutant gonad. Loss of *Dmrt1* affects mRNAs of both Sertoli cells and germ cells. The abnormal expression of these mRNAs indicates defects in several signaling pathways and in differentiation programs likely to underlie the *Dmrt1* mutant phenotype.

Materials and Methods

Germ Cell Radial Movement

Testes were collected from wild type and *Dmrt1*$^{-/-}$ littermates on the day of birth (P0) through P5, fixed in Bouin's fix, followed by dehydration and paraffin embedding, and 7-μm sections were cut and stained with hematoxylin and eosin using standard methods. Germ cells were identified by morphology at these early stages. For each animal, peripheral and central germ cells were counted in 200 seminiferous tubules cut at 90 degrees to the axis of the tubule.

cRNA Preparation and Array Hybridization

P1 and P2 wild type and *Dmrt1*$^{-/-}$ testes were harvested and dissected from epididymis and fat in RNAlater reagent (Ambion). All animals were of mixed background, primarily 129/SvEv and C57BL/6J. For each sample, 5 testis pairs, wild type or *Dmrt1*$^{-/-}$, were pooled and total RNA extracted using Trizol reagent (Invitrogen). RNA was further purified using RNeasy (Qiagen). Double-stranded cDNA was synthesized using the SuperScriptII Reverse Transcription System (Invitrogen). Five to 10 μg of total RNA and 0.34 μM T7-oligo(dT) primer were used for first strand cDNA synthesis. Double-stranded cDNA was purified with GeneChip Sample Cleanup Module (Affymetrix) and transcribed to cRNA using GeneChip IVT Labeling Kit (Affymetrix). Biotinylated cRNA was purified with GeneChip Sample Cleanup Module (Affymetrix) and evaluated by A_{260}:A_{280}. cRNA was fragmented with Fragmentation Buffer (Affymetrix) and hybridized to MGU74Av2 arrays by the University of Minnesota Affymetrix core facility. Four independent arrays were hybridized to pools of wild type and *Dmrt1*$^{-/-}$ cRNA at P1 and P2. CEL (cell intensity) files were used for analysis using the GeneData Expressionist Suite, with quality control implemented using Affymetrix controls. CEL files passing quality guidelines were normalized by Expressionist Refiner reference chip normalization and used to assess and rate the quality of each chip, and to determine outliers. Microarray expression results were visualized using Expressionist Analyst. Summary statistics were applied including histograms, boxplots and principal components analysis. Gene Selection criteria included Genedata Expressionist T-test and fold changes. Fold-change results were based on the ratio of the mean $\log_2$ of each group. Genes with low absolute expression values were not excluded from the analysis.

Real Time RT-PCR

LightCycler-RNA Amplification Kit SYBR Green I kit (Roche Applied Sciences) was used with the Roche LightCycler 2.0 machine. Melting temperatures for each gene specific product were determined using RNA extracted from 10-week-old testes in a standard RNA amplification reaction mix (table 1). RNA was reverse-transcribed at 42°C for 30 min followed by 35 cycles of PCR amplification. PCR conditions were 95°C for 15 s, 20 s at primer T_m, and 15 s at 72°C.

Immunofluorescence and Histology

Testes were fixed either in fresh Ste. Marie's fix (99:1 95% ethanol:glacial acetic acid) (α-occludin) for 1 h or overnight in either Bouins fix (α-Gcna1, α-Sma) or 4% paraformaldehyde at 4°C prior to dehydration and paraffin embedding, depending on the

Table 2. Primers for genotyping

Name	Sequence	Allele detection	T_{PCR} (°C)
CR92	CAGCTCCATGGCGAACGACGACACATTCGG	WT	60[a]
CR99	CTGCAGCGAGCGCATTTGGGCAGC	WT	60[a]
KOS1N	GATCTATCTGGAGCCAGGTGGTAG	KO	65[b]
KOS3N	TCATGGCAGCTCTCCCAGTGGAGC	KO	65[b]

[a] DMSO required.
[b] No DMSO required.

primary antibody used. Sections were cut to 5–7 μm and rehydrated sections were blocked for 1 h with Blocking Buffer (0.2% cold-water fish skin gelatin [Sigma], 5% goat serum and 0.2% Tween 20 in PBS). H2AX and P-H3 antibodies were from Upstate (07–164 and 06–570), Occludin and ZO-1 were from Zymed (71–1500 and 61–7300), and α-smooth muscle actin was from Sigma (A 2547). Gcna1 antibody was a gift from Dr. G. Enders (U. of Kansas Medical Center). Secondary antibodies were Alexa 568 conjugated goat anti-rabbit, Alexa 488 goat anti-mouse, or Alexa 594 goat anti-rat (Molecular Probes) at 1:1,000. For some antibodies antigen unmasking was performed by boiling in 10 mM sodium citrate, pH 6. Primary antibodies were used at 1:1,000 (Dmrt1), undiluted (Gcna1) or at 1:200 dilution.

Imaging

A Bio-Rad Laser Sharp 3.1 system with Kalman collection and 6 passes per Z-step was used to collect images for all figures except figure 5 and figure 6G–I, which used a conventional epifluorescence microscope. Collected confocal images were processed with Confocal Assistant 4.02 and single representative Z sections are shown.

Genotyping

Tail DNA was digested in 500 μl of TENS (50 mM Tris-Cl pH 8, 1 mM EDTA, 20 mM NaCl and 1% SDS) buffer with 192 μg/ml PCR Grade Proteinase K (Roche) at 50°C overnight with rotation. Proteinase K was inactivated at 90°C for 30 min and DNA was diluted 1:100 prior to PCR. Genotyping primers are indicated in table 2.

Results

Postnatal Germ Cell Migration

Shortly after birth, gonocytes migrate from the center to the periphery of the seminiferous tubules, establishing close contact with the basement membrane and neighboring pre-Sertoli cells. This translocation is thought to be important for differentiation of gonocytes into spermatogonia, and is presumed to allow these cells to enter a stem cell niche supportive of spermatogenesis (Ogawa et al., 2005). We found previously that at P7, when wild type germ cells have migrated and are closely juxtaposed with the basement membrane, most *Dmrt1* mutant germ cells are still found in the middle of the seminiferous tubules (Raymond et al., 2000). To determine when this defect first becomes evident, we compared the location of gonocytes in wild type versus *Dmrt1*$^{-/-}$ testes each day from birth to P5 (fig. 1A). At P0 about 10% of germ cells are located at the periphery of the seminiferous tubules of both wild type and *Dmrt1*$^{-/-}$ testes (fig. 1A) and by P1 this increases to about 25% (fig. 1A–C). At P2 there is a clear difference, with about 75% of wild type gonocytes located peripherally (fig. 1A, D), whereas the majority of *Dmrt1*$^{-/-}$ gonocytes remain central (fig. 1A, E). By P5 the translocation is essentially complete in wild type, with more than 90% of the gonocytes located at the periphery, but in *Dmrt1*$^{-/-}$ testes little or no additional translocation occurs (fig. 1A).

Germ Cell Mitosis, Differentiation, and Meiosis

In addition to their radial movement, gonocytes reinitiate mitotic proliferation, differentiate into spermatogonia, and begin to enter meiosis shortly after birth (Vergouwen et al., 1991; Nagano et al., 2000). Previous analysis of *Dmrt1*$^{-/-}$ germ cells showed that they are absent by about P14 (Raymond et al., 2000), but it was unclear whether they initiated any appropriate differentiation prior to their death. We therefore examined markers of mitotic proliferation, differentiation, and meiosis in *Dmrt1* mutant testes and found that these processes are abnormal.

Staining for the mitotic metaphase marker phosphohistone 3 (P-H3) (Hans and Dimitrov, 2001) revealed small numbers of mitotic germ cells beginning at P3 in both wild type and *Dmrt1*$^{-/-}$ seminiferous tubules (data not shown). In wild type, elevated mitosis is clearly evident by P6, and at P7 many germ cells are mitotic

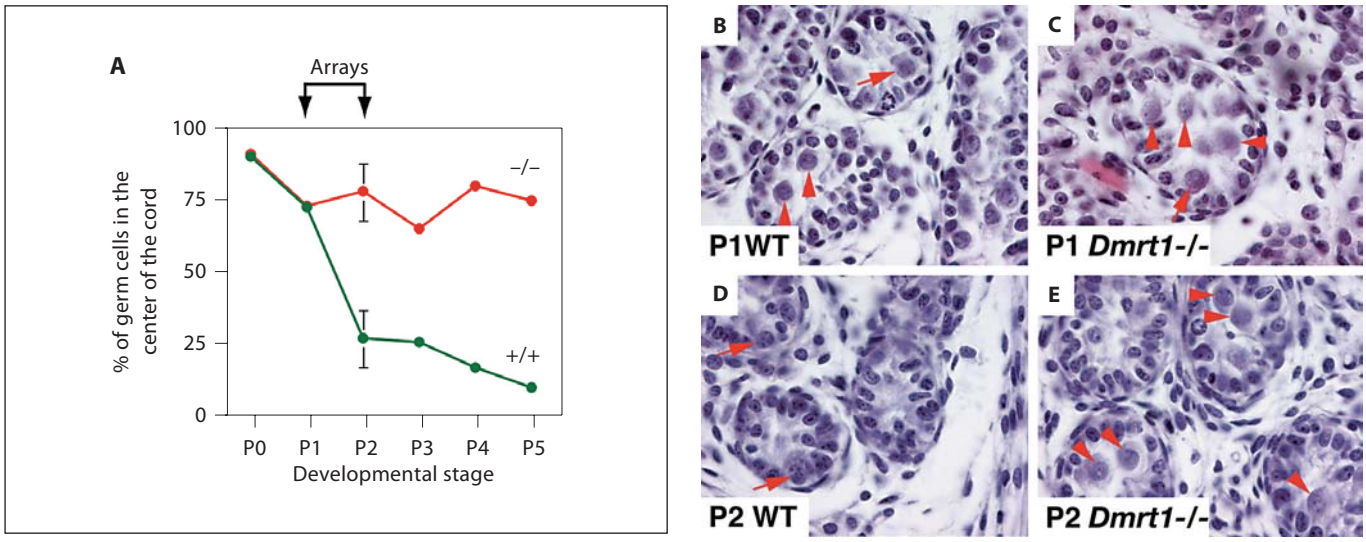

Fig. 1. Defective gonocyte movement in *Dmrt1* mutant testes. **A** Plot of germ cell position in wild type and *Dmrt1*$^{-/-}$ testes between P0 and P5. P0, P1 and P2 values are averaged from testes of 2 animals, with standard deviations shown (visible only for P2). Germ cells were scored as peripheral if any part of the nucleus was within 1 nuclear diameter of the basement membrane; thus the magnitude of the migration defect in the mutant may be somewhat underrepresented. **B–E** H&E staining of seminiferous tubules of wild type and *Dmrt1*$^{-/-}$ animals at P1 and P2. Germ cells in the center of seminiferous tubules are indicated with arrowheads, while those at the periphery are indicated with arrows.

(fig. 2A). Although germ cells are still present in *Dmrt1*$^{-/-}$ testes at this stage, very few are P-H3 positive (fig. 2B). We also examined *Dmrt1*$^{-/-}$ testes at P2, P3, P4 and P6, and confirmed that while a low level of postnatal mitosis occurs, there is no period of elevated mitosis corresponding to that in wild type (data not shown). In principle the deficit in gonocyte mitosis might be a secondary consequence of the defect in radial movement, if localization to the basement membrane is a prerequisite for mitotic reinitiation. We cannot fully exclude this possibility, although previous studies have found that mitotic reinitiation and translocation of gonocytes can occur independently (McGuinness and Orth, 1992; Nagano et al., 2000). Thus the deficits in gonocyte migration and mitosis in the mutant may be, at least in part, separate defects.

To determine whether *Dmrt1*$^{-/-}$ germ cells initiate spermatogonial differentiation or meiosis, we used a phosphorylated H2AX (γ-H2AX) antibody, examining stages from P1 to P7. γ-H2AX is present in intermediate and B spermatogonia, as well as preleptotene to zygotene spermatocytes, and thus it serves as a sensitive marker for germ cell differentiation beyond the gonocyte stage (Hamer et al., 2003). In wild type we observed a sharp increase in γ-H2AX positive germ cells between P4 and P7; in *Dmrt1*$^{-/-}$, by contrast, occasional germ cells express γ-H2AX, but there were much fewer than in wild type (fig. 2C–F and data not shown). Because γ-H2AX also is associated with double-strand DNA breaks in apoptotic cells (Hamer et al., 2003), the γ-H2AX positive germ cells observed in *Dmrt1*$^{-/-}$ testes may be apoptotic rather than differentiating. Consistent with this possibility, some of these cells had nuclear morphology characteristic of apoptosis (fig. 2F). Regardless, *Dmrt1*$^{-/-}$ germ cells clearly do not progress beyond the gonocyte stage in significant numbers.

From the data presented so far we conclude that *Dmrt1* mutant germ cells are deficient for hallmarks of normal postnatal gonocyte development, including migration to the periphery of the seminiferous tubule, elevated postnatal mitosis, and differentiation into spermatogonia and spermatocytes. This suggests that these cells may be developmentally arrested and may more closely resemble embryonic than postnatal germ cells, as discussed further below. The death of *Dmrt1* mutant germ cells may be a consequence of their failure to occupy the spermatogonial niche during a critical period.

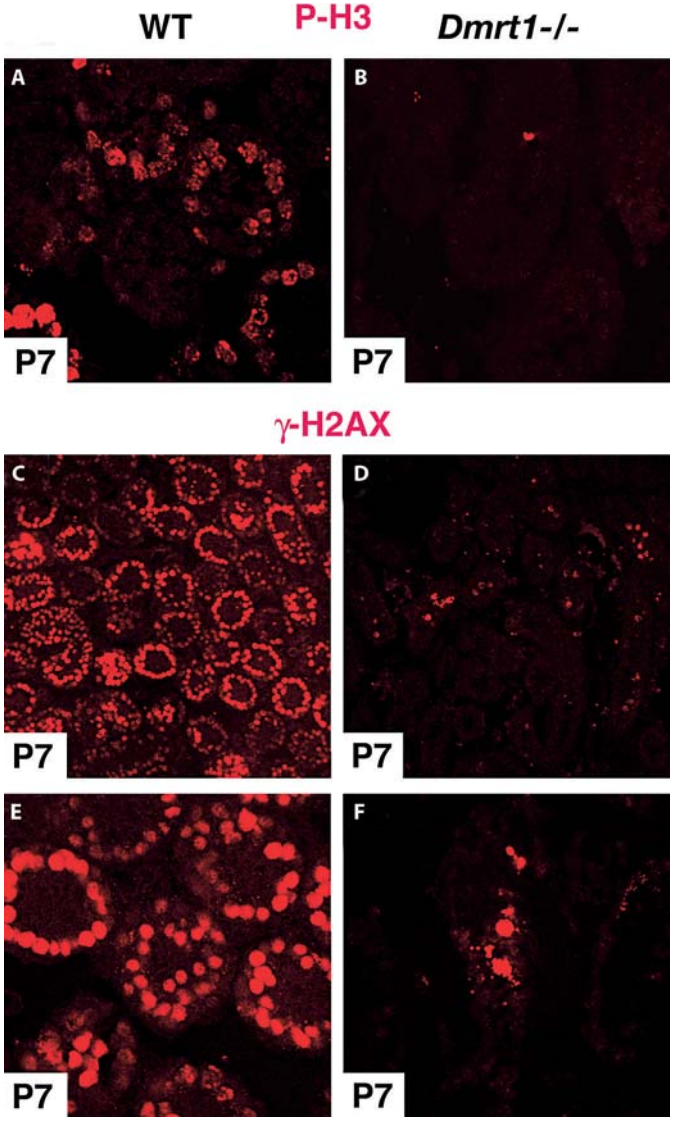

Fig. 2. *Dmrt1*$^{-/-}$ germ cells fail to undergo normal postnatal mitosis and differentiation. **A**, **B** Staining with antibody against the mitotic marker P-H3. **A** P7 wild type, **B** P7 *Dmrt1*$^{-/-}$. **C–F** Staining with antibody against the spermatogonial and meiotic marker γ-H2AX. **C** P7 wild type, **D** P7 *Dmrt1*$^{-/-}$, **E** P7 wild type at higher magnification, **F** P7 *Dmrt1*$^{-/-}$ at higher magnification showing likely apoptotic nuclear morphology in the few cells expressing γ-H2AX.

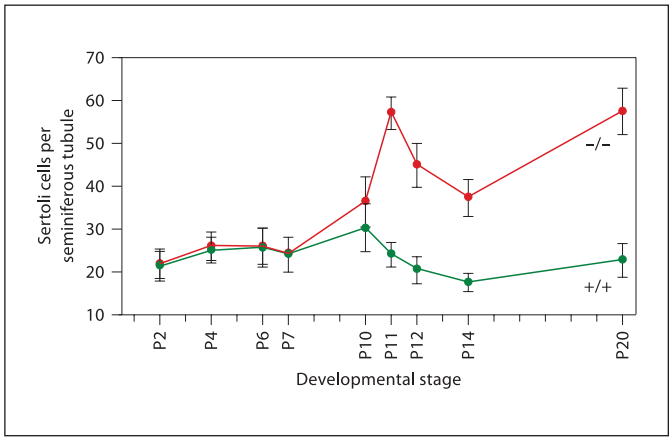

Fig. 3. Supernumerary Sertoli cells in the *Dmrt1*$^{-/-}$ testis. Plot of Sertoli cells present per seminiferous tubule section over time. Red line (–/–) corresponds to *Dmrt1* mutants and green line (+/+) corresponds to WT. Data are from counts of 5 (P20), 10 (P6, P11 and P14), 15 (P4 and P7), or 30 (P10 and P12) seminiferous tubules of each genotype. Tubules from 2 animals were used for P10 through P12. Error bars indicate standard deviation.

Elevated Sertoli Cell Proliferation in Dmrt1$^{-/-}$ *Testis*

Sertoli cell numbers are tightly regulated during testicular differentiation, and the number of Sertoli cells is an important factor for fertility (Orth et al., 1988; Petersen and Soder, 2006). In wild type mice, Sertoli cells cease proliferation by about P15 and undergo maturation (Sharpe et al., 2003; Walker, 2003). We observed previously that *Dmrt1* mutants appear to contain elevated numbers of Sertoli cells from about P14 onward and these appear immature, based on morphology and expression of Gata4 and Gata1 (Raymond et al., 2000). We therefore compared Sertoli cell numbers in wild type and mutant testes from P2 to P20. Because the cross-sectional area of wild type and mutant seminiferous tubules is similar during this period, we counted the number of Sertoli cells per tubule cross-section at each stage (fig. 3). The density of Sertoli cells in wild type and *Dmrt1*$^{-/-}$ seminiferous tubules remains constant from P2 to P7, and by P10 there is a 25% increase in wild type and a 50% increase in *Dmrt1*$^{-/-}$. Between P10 and P20 the number of Sertoli cells decreases slightly in wild type but continues to increase in *Dmrt1*$^{-/-}$, such that by P20 there are nearly three times more Sertoli cells in *Dmrt1*$^{-/-}$ seminiferous tubules than in wild type tubules. These surplus Sertoli cells might result either from excessive proliferation or from reduced apoptosis. However, TUNEL labeling and histological examination revealed no significant difference in apoptosis between mutant and wild type Sertoli cells (not shown). It appears, therefore, that postnatal Sertoli cell proliferation initiates normally in *Dmrt1* mutant testes but does not cease normally, possibly due to a developmental block.

Expression Profiling and Validation

From the phenotypic analysis described above it is clear that *Dmrt1* mutant testes have multiple defects in postnatal differentiation, beginning at or before P2. Dmrt1 is a putative transcriptional regulator, so to identify mRNAs controlled either directly or indirectly by Dmrt1, we profiled mRNAs in wild type versus *Dmrt1*$^{-/-}$ testes using Affymetrix oligonucleotide microarrays. To focus on the earliest expression defects, we examined testes at P1, just before the gonocyte migration defect in *Dmrt1*$^{-/-}$ becomes evident, and at P2, when this phenotype is clearly apparent (fig. 1A).

We performed 4 independent comparisons of wild type versus *Dmrt1*$^{-/-}$ testes at each developmental stage. To minimize expression differences between individuals, each sample contained mRNA from 5 testis pairs. Statistical analysis (see Materials and Methods) identified 64 genes whose expression was reduced by 2-fold or more in mutant testes at P1 or P2 and 54 with expression elevated by 2-fold or more (tables 3 and 4; complete array data are in Supplementary Materials, tables S1 and S2, www.karger.com/doi/1159/000096238). As expected, *Dmrt1* mRNA was strongly reduced in the mutant gonads (17-fold at both stages).

To validate the microarray results we analyzed expression of 8 genes by quantitative RT-PCR (table 1). We chose genes with microarray expression differences in the mutant of at least 2-fold at both P1 and P2. All 6 genes with reduced expression by microarray analysis also had reduced expression by RT-PCR (fig. 4A), and both genes with increased expression by microarray analysis also had increased expression by RT-PCR (fig. 4B). In most cases the magnitude of expression change determined by RT-PCR was similar to or higher than that measured by microarray hybridization. From these results we conclude that the microarray data are likely to accurately identify genes with expression differences, but may underestimate the magnitude of the expression difference for some genes.

Some of the mRNAs identified are likely to be regulated directly and others indirectly by Dmrt1. Dmrt1, like MAB-3 and DSX^{M}, can function as a transcriptional repressor (M.M., unpublished results), and thus the mRNAs with elevated expression in *Dmrt1* mutants are particularly good candidates to be directly regulated. However, more mRNAs show reduced expression, indicating either that they are regulated indirectly or that Dmrt1 also can activate transcription. As a simple test, we made transcriptional reporters, fusing conserved promoter regions of 4 genes to luciferase, and tested whether a fusion protein of Dmrt1 to the VP16 activation domain could activate the reporters in transfected cells. None of the promoters tested (*occludin*, *Stella/Dppa3/Pgc7*, *Hoxa1*, and *Nkx3.1*; data not shown) were activated, indicating either that these are not direct targets or that the Dmrt1 response elements were not present in the 500 to 1,500 bp of upstream sequence tested. Other approaches such as ChIP on chip will be needed to identify the direct targets, and these are under way.

Among the genes we identified by expression profiling are a number of known regulators of testicular development. These include the transcriptional regulator *Dax1* (Swain et al., 1996; Bouma et al., 2005) and signaling components that implicate several pathways (Gdnf, FSH, TGFβ, retinoic acid, and others; see Discussion). We also identified a variety of genes of unknown function that will merit future investigation. Overall, the array data are consistent with the histological data in indicating a broad variety of defects in postnatal testis differentiation. In the following sections we describe expression differences with possible relevance to the germ cell and Sertoli cell defects we observed.

Gonocyte Defects

The PGC marker *Stella/Pgc7/Dppa3* (Saitou et al., 2002; Sato et al., 2002; Bowles et al., 2003; Bortvin et al., 2004) is overexpressed in *Dmrt1* mutant testes at both P1 (4-fold) and P2 (17-fold). *Stella* normally is downregulated in the testis between E16.5 and P1 (Sato et al., 2002), so the failure to downregulate this gene in *Dmrt1* mutants might reflect a block in germ cell differentiation. This would be consistent with the failure of mutant germ cells to undergo the normal postnatal events. We reasoned that if elevated *Stella/Pgc7/Dppa3* is responsible for a block in gonocyte development, reducing its level might relieve the block. To test this idea we generated *Dmrt1; Stella* double mutants. However, the germ cell phenotype of the double mutants closely resembled that of *Dmrt1* single mutants (fig. 5), indicating that elevated *Stella/Pgc7/Dppa3* expression alone cannot be responsible for the apparent developmental arrest. Indeed, other germ cell mRNAs that should show reduced expression after birth are overexpressed in the mutant germ cells, including the PGC marker *nanog* (Yamaguchi et al., 2005) (1.5-fold at P1 and 2-fold at P2) and *Cfl* (Shima et al., 2004) (16-fold at P1 and 11-fold at P2).

Another indication that the PGC to gonocyte transition may be incomplete is reduced expression of *Nkx3.1* mRNA. Nkx3.1 is a homeobox protein expressed predominantly in prostate and testis, and its mRNA was reduced in *Dmrt1*$^{-/-}$ by 5-fold at P1 and 3.5-fold at P2.

Table 3. Genes with at least 2-fold decreased expression in *Dmrt1*$^{-/-}$ testis at P1 or P2

Affymetrix probe set ID	Gene symbol	Gene description	P1 WT	P1 KO	P2 WT	P2 KO	P1 fold change	P2 fold change	P1 t test p value	P2 t test p value
100374_at	*Dmrt1*	doublesex and mab-3 related transcription factor 1	834	60	884	52	16.7	16.8	2.E–04	2.E–06
92907_at	*Ocln*	occludin	227	32	212	19	7.2	12.3	8.E–05	2.E–04
103941_at	*Spna1*	spectrin alpha 1	48	5	72	8	10.3	11.6	6.E–04	4.E–03
99994_at	*Cidea*	cell death-inducing DNA fragmentation factor, alpha subunit-like effector A	376	75	615	75	5.3	8.4	2.E–04	7.E–06
101828_at	*Ret*	ret proto-oncogene	13	4	48	5	2.8	7.3	2.E–02	7.E–04
103296_at	*Cst9* (testatin)	cystatin 9	3,428	1,167	4,405	699	3.1	6.4	2.E–03	6.E–06
103983_at	*Adh4*	alcohol dehydrogenase 4 (class II), pi polypeptide	29	7	28	5	3.9	5.6	3.E–02	1.E–03
104498_at	*Homer1*	homer homolog 1 (Drosophila)	17.5	23.6	22.1	5.18	–1.2	5.1	8.E–01	9.E–03
103982_s_at	*Adh4*	alcohol dehydrogenase 4 (class II), pi polypeptide	13	8	28	5	1.5	5.1	3.E–01	1.E–04
92673_at	*Sh3gl2*	SH3-domain GRB2-like 2	89	29	102	21	3.1	5.0	7.E–04	4.E–04
92425_at	*Chd1l*	chromodomain helicase DNA binding protein 1-like	108	69	137	26	1.5	5.0	2.E–01	6.E–04
94393_r_at	*Elovl2*	elongation of very long chain fatty acids (FEN1/Elo2, SUR4/Elo3, yeast)-like 2	818	296	1,042	253	2.9	4.6	2.E–03	2.E–03
160937_at	*Crym*	crystallin, mu	13.3	9.83	36.8	7.4	1.2	4.3	6.E–01	9.E–03
97941_at	*Capn6*	calpain 6	232	150	339	96	1.5	4.1	1.E–01	5.E–03
101560_at	*Emb*	embigin	261	105	303	75	2.6	4.0	5.E–03	7.E–06
96970_at	*Igh-VS107*	immunoglobulin A heavy chain variable region (IGHV gene), clone AJ3	29	40	113	32	–1.4	3.8	6.E–01	6.E–03
97157_at	*Nkx3-1*	NK-3 transcription factor, locus 1 (Drosophila)	214	47	216	61	5.1	3.5	3.E–03	9.E–06
99845_at	*Slc1a6*	solute carrier family 1 (high affinity aspartate/glutamate transporter), member 6	468	130	431	126	4.2	3.5	7.E–03	3.E–04
103213_at	*Cdh15*	cadherin 15	73	44	63	19	1.6	3.3	1.E–01	5.E–05
162277_r_at	*Polg2*	polymerase (DNA directed), gamma 2, accessory subunit	11.8	20	18.8	6.4	–1.9	3.2	2.E–01	5.E–03
93259_at	*Tnnc2*	troponin C2, fast	6.98	5.9	9.88	3.33	1.2	3.2	6.E–01	6.E–03
98123_at	*Aadat*	aminoadipate aminotransferase	12.7	18	20	6.58	–1.9	3.2	2.E–01	8.E–03
102661_at	*Egr2*	early growth response 2	243	117	298	95	2.1	3.2	2.E–03	7.E–06
160953_at	*Cacna1h*	calcium channel, voltage-dependent, T type, alpha 1H subunit	36	34	46	16	1.1	3.0	6.E–01	3.E–03
94772_at	*Klrb1a*	killer cell lectin-like receptor subfamily B member 1A	36	39	41	14	–1.1	3.0	1.E+00	7.E–03
101918_at	*Tgfb1*	transforming growth factor, beta 1	86	17	68	23	4.2	2.9	1.E–02	7.E–02
96704_at	*Sfn*	stratifin	208	75	274	100	2.7	2.9	1.E–03	9.E–03
104257_g_at	*Pscdbp*	pleckstrin homology, Sec7 and coiled/coil domains, binding protein	442	204	522	181	2.2	2.9	7.E–05	8.E–06
104646_at	*Gdf15 (MIC-1)*	growth differentiation factor 15	290	86	223	81	3.4	2.8	2.E–04	7.E–03
99056_at	*Pcbd1*	pterin 4 alpha carbinolamine dehydratase/dimerization cofactor of hepatocyte nuclear factor 1 alpha (TCF1) 1	259	137	258	94	1.9	2.8	9.E–04	4.E–05
92932_at	*Cbln1*	cerebellin 1 precursor protein	1,542	529	1,377	512	3.0	2.7	3.E–04	7.E–05
100768_at	*?*	?	26.2	8.75	21.1	6.35	3.1	2.6	9.E–04	1.E–01
97520_s_at	*Nnat*	neuronatin	1,019	379	918	363	2.7	2.5	7.E–04	2.E–05
161963_f_at		RIKEN cDNA C330007P06 gene	36	50	49	19	–1.4	2.5	5.E–01	4.E–03
97942_g_at	*Capn6*	calpain 6	1,821	1,057	2,225	894	1.7	2.5	2.E–02	5.E–04
160863_at	*Tulp2*	tubby-like protein 2	420	192	513	208	2.2	2.5	2.E–04	1.E–05

Table 3 (continued)

Affymetrix probe set ID	Gene symbol	Gene description	P1 WT	P1 KO	P2 WT	P2 KO	P1 fold change	P2 fold change	P1 t test p value	P2 t test p value
93872_at	*Gfra1*	glial cell line derived neurotrophic factor family receptor alpha 1	94	45	146	61	2.1	2.4	1.E–02	3.E–03
102737_at	*Edn1*	endothelin 1	280	142	325	137	2.0	2.4	9.E–05	3.E–04
98440_at		RIKEN cDNA 2510002C21 gene (Ltb4dh)	3,221	1,782	3,829	1,603	1.8	2.4	3.E–05	7.E–05
102557_at		Cluster Incl U62673: *Mus musculus* histone H2a(A)-613, histone H2a(B)-613, and histone H2b-613 (H2b) genes	66	73	95	40	–1.1	2.4	5.E–01	9.E–03
97943_at	*Capn6*	calpain 6	1,277	867	1,594	685	1.5	2.3	3.E–03	7.E–04
97317_at	*Enpp2*	ectonucleotide pyrophosphatase/phosphodiesterase 2	549	372	611	261	1.5	2.3	1.E–02	9.E–04
92374_at	*Adora1*	adenosine A1 receptor	323	139	332	143	2.4	2.3	3.E–03	7.E–04
95940_f_at		cDNA sequence BC052328	146	67	161	70	2.2	2.3	5.E–03	5.E–04
98007_at	*Rps6ka2*	ribosomal protein S6 kinase, 90kD, polypeptide 2	514	296	597	271	1.9	2.2	3.E–03	2.E–04
103755_at	*Sh3d19*	SH3 domain protein D19	253	145	524	200	1.7	2.2	6.E–02	3.E–03
101412_at	*Sh3gl3*	SH3-domain GRB2-like 3	913	383	764	354	2.4	2.2	3.E–06	3.E–03
102652_at	*Pou3f1*	POU domain, class 3, transcription factor 1	39	31	53	25	1.3	2.1	6.E–01	4.E–03
93285_at	*Dusp6*	dual specificity phosphatase 6	1,619	933	1,701	822	1.7	2.1	4.E–03	1.E–03
160795_at	*Scamp1*	secretory carrier membrane protein 1	291	190	301	148	1.5	2.1	4.E–03	7.E–03
104256_at	*Pscdbp*	pleckstrin homology, Sec7 and coiled/coil domains, binding protein	88	59	111	53	1.5	2.1	5.E–02	8.E–04
95655_at		RIKEN cDNA 4930434H03 gene	298	201	412	192	1.5	2.1	2.E–01	9.E–04
92184_at	*Dtna*	dystrobrevin alpha	155	96	190	86	1.1	2.1	1.E–02	9.E–03
101810_at	*Fshr*	follicle stimulating hormone receptor	864	412	963	473	2.1	2.0	4.E–04	3.E–04
160500_at	*Atp1b1*	ATPase, Na^+/K^+ transporting, beta 1 polypeptide	66	62	79	38	1.1	2.0	8.E–01	3.E–03
102859_at	*?*	DNA segment, Chr 6, ERATO Doi 253, expressed	3,567	1,829	3,881	1,926	2.0	2.0	8.E–04	2.E–04
93604_f_at	*Igsf4a*	immunoglobulin superfamily, member 4	2,044	1,072	1,689	833	1.9	2.0	7.E–03	1.E–05
93141_at	*Nr0b1 (Dax1)*	nuclear receptor subfamily 0, group B, member 1	850	483	1,190	594	1.8	2.0	5.E–03	1.E–04
104432_at	*Rnd2*	Rho family GTPase 2	971	526	1,056	524	1.9	2.0	5.E–03	3.E–04
92901_at	*Rara*	retinoic acid receptor, alpha	322	153	290	163	2.1	1.8	4.E–03	3.E–02
99957_at	*Mmp9*	matrix metalloproteinase 9	124	33	107	72	4.2	1.5	8.E–03	3.E–01
100403_at	*Myl7*	myosin, light polypeptide 7, regulatory	58	24	38	30	2.4	1.2	9.E–03	5.E–01
98126_s_at	*Atp2a1*	ATPase, Ca++ transporting, cardiac muscle, fast twitch 1	93	35	76	61	2.8	1.2	8.E–03	4.E–01
98311_at	*Pmfbp1*	polyamine modulated factor 1 binding protein 1	55.9	14.1	37.2	37.6	3.9	–1.0	3.E–03	1.E+00

Affymetrix probe set IDs are for the MGU74Av2 chip. P1 and P2 wild type (WT) and Dmrt1 knockout (KO) values are the average of 4 independent sample preparations and hybridizations. Fold changes and t test p values were calculated using Genedata Expressionist Software. Genes with at least a 2-fold change in expression from WT and a t test of 0.01 or less are shown. The complete data set is provided online as Supplementary Tables S1 and S2, www.karger.com/doi/10.1159/000096238.

Microarrays detect *Nkx3.1* mRNA predominantly during the first 14 days of postnatal development, and type A spermatogonia were the highest expressing adult testis cell type assayed (Shima et al., 2004). *Nkx3.1* homozygotes are viable but have reduced fertility (C. Abate-Shen, pers. comm.). We examined *Nkx3.1* mutant testes histologically, but did not observe any defects in cellular organization or spermatogenesis (data not shown). We con-

Table 4. Genes with at least 2-fold increased expression in *Dmrt1*$^{-/-}$ testis at P1 or P2

Affymetrix probe set ID	Gene symbol	Gene description	P1 WT	P1 KO	P2 WT	P2 KO	P1 fold change	P2 fold change	P1 t test p value	P2 t test p value
97283_at	*Dppa3 (Stella)*	developmental pluripotency-associated 3	26	136	11	187	3.6	17.0	3.E–04	2.E–03
99927_at	*Cfi*	complement component factor i	18	275	21	235	15.5	11.2	1.E–04	2.E–03
98034_at	*H2-DMb1*	histocompatibility 2, class II, locus Mb1	5	37	3	29	6.5	9.8	5.E–03	7.E–04
100998_at	*H2-Ab1*	histocompatibility 2, class II antigen A, beta 1	86	260	29	229	3.0	7.9	1.E–02	2.E–06
97379_at	*Fbp2*	fructose bisphosphatase 2	17	27	7	36	1.3	5.3	6.E–01	3.E–04
92866_at	*H2-Aa*	histocompatibility 2, class II antigen A, alpha	91	340	65	312	4.2	4.8	3.E–03	2.E–03
100127_at	*Crabp2*	cellular retinoic acid binding protein II	85	197	67	325	2.3	4.6	1.E–04	3.E–04
102900_at	*Six3, E130112 M24Rik*	sine oculis-related homeobox 3 homolog (Drosophila) RIKEN cDNA E130112M24 gene	8	9	4	19	1.2	4.6	8.E–01	6.E–03
96504_at	*Pax8*	paired box gene 8	62	93	26	109	1.5	4.2	4.E–01	2.E–03
160606_r_at	*Adamts1*	a disintegrin-like and metalloprotease (reprolysin type) with thrombospondin type 1 motif, 1	13	16	8	32	1.3	4.1	4.E–01	4.E–03
95297_at	*Hoxa1*	homeo box A1	3	10	3	12	3.2	4.0	4.E–04	6.E–04
96931_at	*Mrp63*	mitochondrial ribosomal protein 63	24	29	12	48	1.3	4.0	9.E–01	6.E–03
100675_at	*Gabrr1*	gamma-aminobutyric acid (GABA-A) receptor, subunit rho 1	15	35	9	32	3.1	3.5	9.E–02	3.E–03
104457_at	*Vps13c*	vacuolar protein sorting 13C (yeast)	18	17	11	32	–1.1	3.5	9.E–01	8.E–03
101289_f_at	*Klk22*	kallikrein 22	47	61	24	75	1.3	3.1	2.E–01	8.E–03
104175_at	*Dlgh4*	discs, large homolog 4 (Drosophila)	56	49	21	67	–1.1	3.1	9.E–01	2.E–04
99449_at	*Kcnq2*	potassium voltage-gated channel, subfamily Q, member 2	92	86	26	86	–1.1	3.0	7.E–01	8.E–03
103548_at	*Tac2*	tachykinin 2	62	101	30	80	1.6	2.9	1.E–01	9.Ev03
102238_at	*Ascl1*	achaete-scute complex homolog-like 1 (Drosophila)	31	60	21	62	1.9	2.9	1.E–01	6.E–04
93354_at	*Apoc1*	apolipoprotein C-I	353	746	272	775	2.1	2.8	5.E–03	7.E–04
100322_at		Gene model 1409, (NCBI) (Gm1409), mRNA	36	50	23	59	1.4	2.8	2.E–01	8.E–03
160810_r_at		RIKEN cDNA 2510022D24 gene	100	90	56	153	–1.1	2.7	1.E+00	2.E–03
96000_at	*Atp6v0a1*	ATPase, H+ transporting, lysosomal V0 subunit A1	8	9	4	10	1.1	2.7	6.E–01	1.E–02
94156_at	*Nppc*	natriuretic peptide precursor type C	49	101	41	106	2.1	2.7	4.E–03	5.E–03
160868_at	*Rab3b*	RAB3B, member RAS oncogene family	51	168	76	198	3.2	2.6	9.E–03	1.E–02
93800_f_at	*Krt1-c29*	keratin complex-1, acidic, gene C29	107	168	72	185	1.6	2.6	8.E–02	2.E–03
94285_at	*H2-Eb1*	histocompatibility 2, class II antigen E beta	222	567	172	429	2.5	2.4	1.E–03	1.E–03
101777_at	*Erbb4*	v-erb-a erythroblastic leukemia viral oncogene homolog 4 (avian)	18	14	15	37	–1.4	2.3	3.E–01	8.E–03
104486_at	*A2m*	alpha-2-macroglobulin	59	126	45	105	2.1	2.3	7.E–03	3.E–02
97783_at	*Ccl17*	chemokine (C-C motif) ligand 17	2,657	3,228	1,094	2,582	1.2	2.3	4.E–01	2.E–03
98035_g_at	*H2-DMb1*	histocompatibility 2, class II, locus Mb1	129	185	101	231	1.5	2.3	3.E–02	2.E–04
98853_at	*Pla2g1br*	phospholipase A2, group IB, pancreas, receptor	41	55	27	60	1.3	2.2	2.E–01	1.E–03
103776_at	*AI593864*	expressed sequence AI593864	27	45	17	37	1.8	2.2	2.E–01	7.E–03
95024_at	*Usp18*	ubiquitin specific protease 18	19	46	15	30	2.4	2.1	2.E–01	7.E–03
101009_at	*Krt2-8*	keratin complex 2, basic, gene 8	408	944	478	984	2.3	2.1	6.E–05	1.E–03
100772_g_at	*Blnk*	B-cell linker	46	71	45	94	1.6	2.1	4.E–02	2.E–03
102393_at	*Cryaa*	crystallin, alpha A	49	48	33	71	–1.0	2.1	9.E–01	4.E–03
99332_at	*Oprd1*	opioid receptor, delta 1	14	17	9	19	1.1	2.1	9.E–01	5.E–03
162194_r_at	*Pkp2*	plakophilin 2	5	14	10	19	3.0	2.0	2.E–03	9.E–02

Table 4 (continued)

Affymetrix probe set ID	Gene symbol	Gene description	P1 WT	P1 KO	P2 WT	P2 KO	P1 fold change	P2 fold change	P1 t test p value	P2 t test p value
97427_at	*Mbl2*	mannose binding lectin, serum (C)	44	64	44	90	1.5	2.0	6.E–02	9.E–04
102344_s_at	*Tcea3*	transcription elongation factor A (SII), 3	109	197	101	202	1.8	2.0	3.E–04	9.E–04
104344_at	*Klkb1*	kallikrein B, plasma 1	28	74	50	99	2.8	2.0	9.E–03	1.E–02
160899_at	*Pcp4*	Purkinje cell protein 4	40	90	40	74	2.2	1.8	5.E–03	3.E–02
94049_at	*Bhmt*	betaine-homocysteine methyltransferase	15	43	36	52	2.9	1.5	4.E–04	2.E–01
97781_at	*Ncr1*	natural cytotoxicity triggering receptor 1	5	11	9	11	2.4	1.5	2.E–03	6.E–01
99863_at	*Slc7a6*	solute carrier family 7 (cationic amino acid transporter, y + system), member 6	9	29	27	34	3.2	1.4	2.E–03	4.E–01
101463_at	*Apoc4*	apolipoprotein C-IV	24	58	36	48	2.4	1.4	3.E–04	3.E–01
103649_at	*Hao3*	hydroxyacid oxidase (glycolate oxidase) 3	368	751	664	843	2.1	1.3	4.E–03	5.E–02
102612_at	*Nrl*	neural retina leucine zipper gene	6	25	23	17	4.1	–1.1	8.E–03	8.E–01
94391_at	*Gjb6*	gap junction membrane channel protein beta 6	6	24	13	9	5.0	–1.1	6.E–03	9.E–01
102906_at	*Tgtp*	T-cell specific GTPase	9	34	17	12	3.7	–1.3	8.E–03	6.E–01
101880_at	*Col18a1*	procollagen, type XVIII, alpha 1	20	53	37	20	2.6	–1.8	6.E–03	3.E–02
161394_f_at	*Hist1h2bp*	histone 1, H2bp	5	23	15	7	4.4	–2.0	8.E–04	7.E–02
102089_at	*Matn3*	matrilin 3	5	24	26	6	5.0	–3.0	1.E–03	9.E–02

Data is as described in Table 3. The complete data set is provided online as supplementary Tables S1 and S2, www.karger.com/doi/10.1159/000096238.

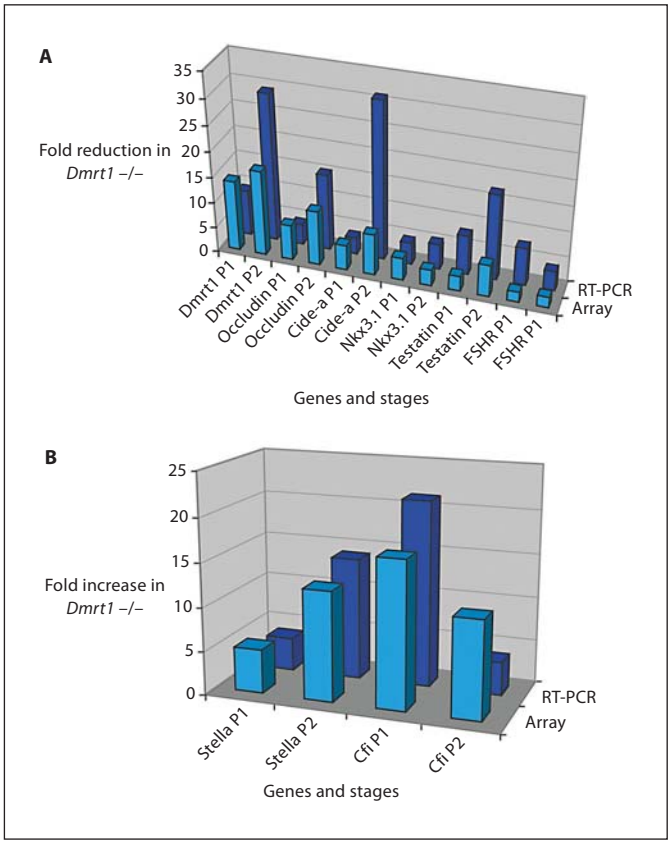

clude that *Nkx3.1* may contribute to the *Dmrt1* mutant phenotype in concert with other misregulated genes, but it is not strongly required for testis development or function. Instead it is possible that the impaired prostate development in *Nkx3.1* mutants (Bhatia-Gaur et al., 1999) may account for their reduced fertility.

Matrix metalloproteases have been implicated in a variety of cell migrations, and the family member *Mmp9* showed reduced expression in *Dmrt1* mutant testes. Mmp9 has been shown to process Kit ligand, allowing recruitment of hematopoietic stem cells to a proliferative niche (Heissig et al., 2002). We reasoned that Mmp9 might play a similar role in recruitment of gonocytes to the spermatogenic niche, and that lack of *Mmp9* might be responsible for the inability of germ cells to migrate radially in *Dmrt1* mutants. To test this idea we exam-

Fig. 4. Validation of microarray mRNA expression by quantitative RT-PCR. **A** Comparison of fold reduction at P1 and P2 for six mRNAs measured by array hybridization (light blue) and quantitative RT-PCR (dark blue). **B** Comparison of fold increase at P1 and P2 for 2 mRNAs measured by array hybridization (light blue) and quantitative RT-PCR (dark blue).

ined testes of *Mmp9* homozygous null mutants (provided by Z. Werb, UCSF). Although these mutants are subfertile (Z. Werb, pers. comm.), *Mmp9* mutant gonocyte migration appeared normal at P5 based on hematoxylin/eosin and Gcna1 antibody staining (not shown). From this we conclude that *Mmp9* is not essential for postnatal gonocyte migration and its lower expression is not the primary cause of failed migration in the *Dmrt1* mutant. It is possible that *Mmp9* has no role in this process or that it functions redundantly with another family member.

Sertoli Cell Tight Junction Formation

The most strongly reduced mRNA in *Dmrt1* mutant testes at P2 is that of *occludin*, which encodes an integral membrane component of tight junctions (Cyr et al., 1999; Schneeberger and Lynch, 2004). Tight junction formation is a key event in Sertoli cell maturation, and tight junctions have been proposed to serve a variety of functions. These include helping to polarize the Sertoli

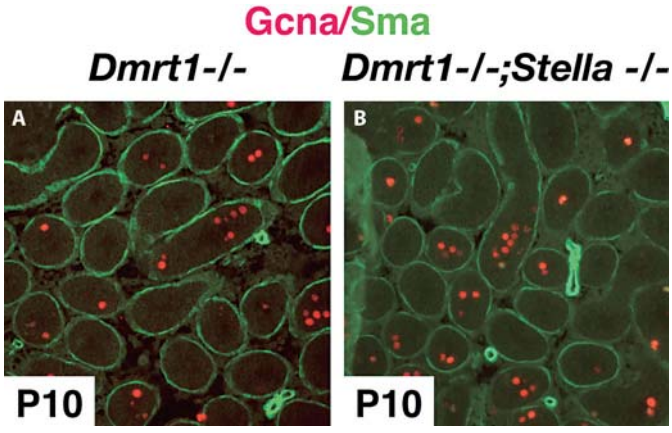

5

Fig. 5. Germ cells in *Dmrt1* versus *Dmrt1;Stella* double mutants. Staining with antibody to germ cell marker Gcna (red) and antibody to the peritubular myoid cell marker smooth muscle actin (Sma; green). **A** *Dmrt1* mutant testis at P10. **B** *Dmrt1;Stella* double mutant testis at P10.

Fig. 6. Lack of occludin expression in *Dmrt1* mutant seminiferous tubules. **A–F** Staining with antibody to occludin. **G–I** staining with antibodies to occludin and Sma. **A**, **B** Staining of occludin is punctate at P2, with lower levels in *Dmrt1* mutant. **C**, **D** By P14 occludin is organized into junctions in wild type but not in *Dmrt1* mutant. **E**, **F** At P20 junctions are fully formed in wild type and no expression of occludin is detectable in *Dmrt1* mutant. **G–I** At P36, normal tight junctions are present in wild type and in the germ cell deficient mutant *c-kit*$^{W/Wv}$, but no occludin expression is detectable in *Dmrt1* mutant.

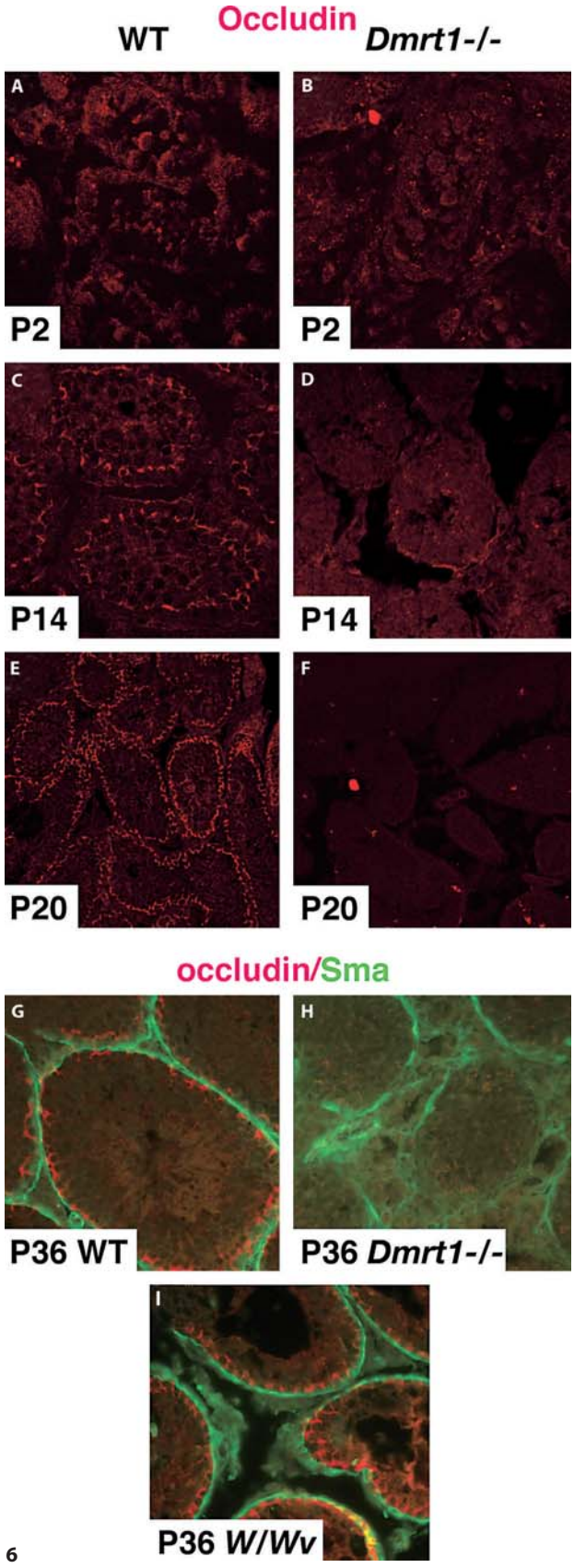

6

cell, establishing the blood-testis barrier, and regulating cell signaling (reviewed in Cheng and Mruk, 2002). We examined occludin expression and organization in *Dmrt1*$^{-/-}$ testes starting at P2 and extending through the period during which tight junctions normally form (fig. 6). In wild type testes at P2, occludin protein is mostly detected in Sertoli cell and gonocyte cytoplasm. Expression in *Dmrt1*$^{-/-}$ seminiferous tubules is similar but reduced, consistent with our microarray and RT-PCR data. At P14 tight junctions are apparent in wild type (fig. 6C). However, while diffuse staining and small puncta of occludin were present in mutant testes, there was no organization into higher order structures resembling those of wild type (fig. 6D). By P20, tight junctions were fully formed in wild type, whereas no occludin was detectable in *Dmrt1*$^{-/-}$ testes (fig. 6E, F). *Dmrt1* mutant testes lose germ cells at the time when tight junctions should form. To test whether lack of germ cells might cause the junctional defect, we examined occludin expression in *c-kit*$^{W/Wv}$ mutant testes, which lack germ cells (fig. 6G–I). We found that junctions containing occludin formed normally in these mutants, indicating that the lack of occludin-containing junctions in *Dmrt1* mutants is likely a Sertoli cell-autonomous defect.

Tight junctions can form in the absence of occludin (Saitou et al., 2000). To determine whether tight junctions lacking occludin can form in *Dmrt1* mutant testes, we examined 2 other proteins, the tight junction associated protein ZO-1 (Byers et al., 1991; Yan and Cheng, 2005), and the integral membrane protein claudin-11, which is crucial for testis tight junction formation (Gow et al., 1999; Bronstein et al., 2000). ZO-1 protein was localized to tight junctions in wild type by P14 (fig. 7A, C, E). In *Dmrt1*$^{-/-}$ testes, aggregated ZO-1 protein was detectable and the expression level was similar to that of wild type, but it was not organized into continuous tight junctions near the tubule periphery like those of wild type. Instead the aggregates were concentrated mainly in the center of the tubules (fig. 7B, D, F). The ZO-1 aggregates may be Sertoli/Sertoli adherens junctions, another structure in which ZO-1 is found (Byers et al., 1991; Schneeberger and Lynch, 2004) or may be incomplete tight junctions. Expression of claudin-11 also indicated a

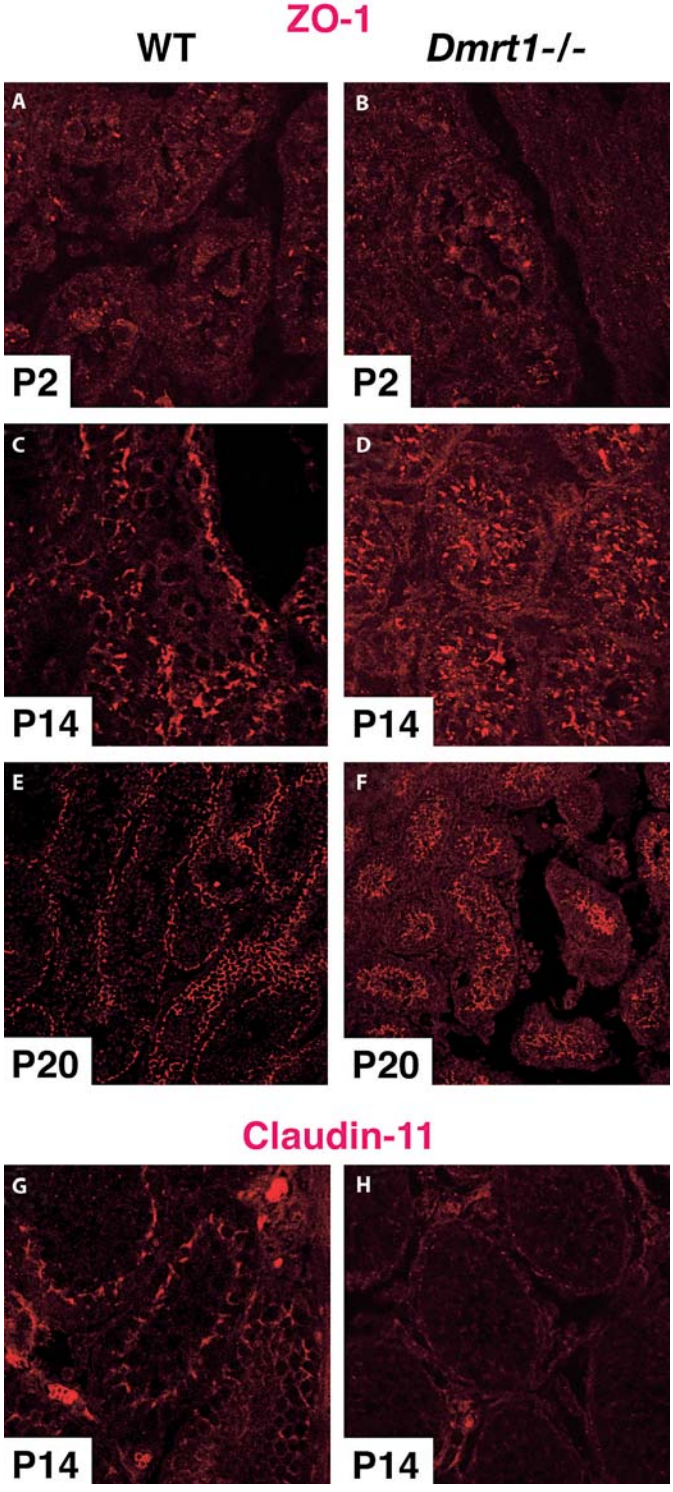

Fig. 7. Abnormal junctional organization in *Dmrt1* mutant seminiferous tubules. **A–F** Staining with antibody to junction-associated protein ZO-1 (wild type in left column and *Dmrt1*$^{-/-}$ in right column). ZO-1 staining is diffuse at P2 in wild type and *Dmrt1*$^{-/-}$ seminiferous tubules. At P14 and P20, ZO-1 is localized to tight junctions in WT. In *Dmrt1*$^{-/-}$ seminiferous tubules at this stage, ZO-1 is present in aggregates, but these are mainly in the center of the tubules, rather than near the periphery. **G**, **H** Staining with antibody to junctional protein Claudin-11.

failure of tight junction formation: at P14 claudin-11 was localized to tight junctions in wild type, but no such localization was detectable in *Dmrt1*$^{-/-}$ testes (fig. 7G versus H). Together these data indicate that *Dmrt1* mutant testes fail to form Sertoli cell tight junctions, possibly as a consequence of a developmental arrest like that we propose for the germ cells. Failure to induce expression of tight junction components may be one factor contributing to the failure of Sertoli cell polarization in *Dmrt1* mutants.

Discussion

Here we have extended earlier studies of *Dmrt1* in the mouse using more detailed phenotypic analysis paired with mRNA expression profiling in *Dmrt1* mutant testes. We find that phenotypic defects in *Dmrt1* mutants include gonocyte migration, gonocyte proliferation, meiotic initiation, Sertoli cell proliferation, and Sertoli cell differentiation, and that these start to become apparent within 2 days after birth. Expression profiling identified ~120 mRNAs whose expression is significantly reduced or elevated at P1 or P2, providing a suite of candidate effectors of *Dmrt1* function for further investigation.

Among the proteins implicated by these studies are components of several important testicular signaling pathways, markers of pluripotent germ cells, Sertoli cell junctional proteins, and class II MHC proteins, as well as a number of proteins whose significance is not yet clear. Some of the expression changes in the mutant testis are likely to be indirect consequences of the arrested developmental progression caused by loss of *Dmrt1*, while others may more directly indicate defects in processes controlled by *Dmrt1*, as discussed below.

Signaling Pathway Abnormalities

Abnormal expression of genes involved in several testicular signaling pathways may contribute to the observed defects in *Dmrt1*$^{-/-}$ germ cells. In particular, signaling by Glial cell line-derived neurotrophic factor (Gdnf) is likely to be compromised. Expression of both Gdnf co-receptors, *Ret* and *Gfra1*, was reduced at P1 and P2. *Gdnf* activity is critical for maintenance of germ line stem cells: heterozygosity of *Gdnf* leads to depletion of stem cells, while over-expression in transgenic animals causes accumulation of undifferentiated spermatogonia (Meng et al., 2000; Tadokoro et al., 2002). FSH receptor mRNA also was under-expressed. This may have similar phenotypic consequences, as FSH signaling has been implicated in increasing *Gdnf* expression (Tadokoro et al., 2002).

We also identified two potential defects in retinoic acid signaling: *CrabpII* mRNA, which encodes a retinoic acid binding protein, was elevated in *Dmrt1*$^{-/-}$ testis, while retinoic acid receptor-α mRNA was reduced. The likely consequence of these changes for retinoic acid signaling is unclear, as they are predicted to have opposite effects. CrabpII can interact with RAR/RXR heterodimers and act as a transcriptional coactivator (Delva et al., 1999; Dong et al., 1999), and this might potentially increase the strength of retinoic acid signaling. However, reduced RARα might compromise this effect. Retinoic acid signaling triggers meiotic entry in both sexes, and sexual dimorphism in meiotic entry is due to male-specific inhibition of this process in the embryo (Bowles et al., 2006; Koubova et al., 2006). Aberrant expression of *RARα* and *CrabpII* may contribute to the complete failure to enter meiosis in *Dmrt1* mutant testes, either by reducing the meiotic entry signal or by providing an elevated signal at an inappropriate time.

Expression profiling also may implicate two other signaling pathways. We detected reduced expression of *Ltb4dh*, a Sertoli cell specific prostaglandin catabolic enzyme (Tai et al., 2002; Shima et al., 2004), suggesting a possible defect in prostaglandin or other eicosinoid signaling. We also detected elevated expression of *tachykinin 2*, which encodes a secreted peptide thought to modulate Leydig and Sertoli cell function (Debeljuk et al., 2003).

Arrested Development of Dmrt1 *Mutant Cells*

Some of the mRNA expression changes we observed in *Dmrt1* mutant testes are consistent with a developmental arrest involving germ cells and Sertoli cells, and this is consistent with our histological analysis of the mutant phenotype. Among the mRNAs detected was the germ cell pluripotency marker *Stella/Dppa3/Pgc7*. In addition to suggesting a block in the progression of gonocyte differentiation, this suggests the possibility that *Dmrt1* mutant germ cells may retain inappropriate pluripotent potential. Indeed, we have found, in work to be described elsewhere, that *Dmrt1* loss of function can result in testicular teratoma formation (T. Krentz, S. Kim, V.B. and D.Z., unpublished).

As described earlier, we genetically tested the potential contributions of several of the misregulated genes (*Dppa3*, *Nkx3.1*, *Mmp9*) to the *Dmrt1* mutant phenotype, but did not observe any significant defects. Their lack of

individual phenotypes excludes these genes as being individually required for aspects of testis development controlled by *Dmrt1*. It is likely that some features of the *Dmrt1* phenotype result from the combined misregulation of multiple genes, possibly including those we tested individually.

MHC Class II Gene Overexpression

Dmrt1 mutant testes had increased expression of several MHC type II mRNAs as well as invariant chain mRNA, which encode proteins involved in antigen presentation. This suggests either elevated numbers or abnormal activation of antigen presenting cells such as macrophages. Sertoli cells are thought to play a role in suppression of testicular macrophages, helping to direct them to produce anti-inflammatory cytokines and promote testicular function (Hedger, 2002). The elevated expression of mRNAs involved in antigen presentation may represent a failure of Sertoli cells to prevent macrophage activation. Consistent with such a model, we detected reduced expression of two potential inhibitors of macrophage activation, *Tgfβ1* and *Mic1* (Fairlie et al., 1999) and increased expression of the TGFβ1 antagonist alpha2 macroglobulin (Arandjelovic et al., 2003). The normal functions of testicular macrophages are poorly understood, but may include stimulation of Leydig cell steroidogenesis (Hedger, 1997). A defect in macrophage function might therefore lead to Leydig cell misfunction, and indeed we have observed that *Dmrt1* mutant males are incompletely virilized (J. Balciuniene, unpublished data).

Conclusion

Dmrt1 mutant testes have a number of defects in early postnatal differentiation, involving multiple cell types, and we identified a variety of misexpressed mRNAs in the mutant testis during this period. Taken together, the phenotypic and molecular data reported here suggest that *Dmrt1* plays an important role in coordinating the transition from embryonic to postnatal testicular differentiation. Many of the misexpressed genes we identified clearly fall into known pathways or processes and provide insight into the etiology of testicular dysgenesis in the mutant testis. The relevance of others is less obvious, but these mRNAs, which encode a wide range of proteins, should provide useful entry points to better understand testicular differentiation.

Acknowledgements

We thank Dr. Alex Bortvin for providing *Dppa3* mutant mice, Drs. Zena Werb and Ying Yu for providing *Mmp9* mutant testes, Dr. George Enders for Gcna1 antibody, Suzanne Grindle for assistance in microarray data analysis, the University of Minnesota Supercomputing Institute for software, and Dr. Cory Abate-Shen and members of the Zarkower and Bardwell laboratories for helpful discussions. *Nkx3.1* mutant mice were provided by the NCI Mouse Models of Human Cancers Consortium repository at NCI-Frederick.

References

Arandjelovic S, Freed TA, Gonias SL: Growth factor-binding sequence in human alpha2-macroglobulin targets the receptor-binding site in transforming growth factor-beta. Biochemistry 42:6121–6127 (2003).

Baker BS, Ridge KA: Sex and the single cell. I. On the action of major loci affecting sex determination in *Drosophila melanogaster*. Genetics 94:383–423 (1980).

Bhatia-Gaur R, Donjacour AA, Sciavolino PJ, Kim M, Desai N, et al: Roles for Nkx3.1 in prostate development and cancer. Genes Dev 13:966–977 (1999).

Bortvin A, Goodheart M, Liao M, Page DC: *Dppa3/Pgc7/stella* is a maternal factor and is not required for germ cell specification in mice. BMC Dev Biol 4:2 (2004).

Bouma GJ, Albrecht KH, Washburn LL, Recknagel AK, Churchill GA, Eicher EM: Gonadal sex reversal in mutant *Dax1* XY mice: a failure to upregulate *Sox9* in pre-Sertoli cells. Development 132:3045–3054 (2005).

Bowles J, Teasdale RP, James K, Koopman P: Dppa3 is a marker of pluripotency and has a human homologue that is expressed in germ cell tumours. Cytogenet Genome Res 101: 261–265 (2003).

Bowles J, Knight D, Smith C, Wilhelm D, Richman J, et al: Retinoid signaling determines germ cell fate in mice. Science 312:596–600 (2006).

Brennan J, Capel B: One tissue, two fates: molecular genetic events that underlie testis versus ovary development. Nat Rev Genet 5: 509–521 (2004).

Bronstein JM, Chen K, Tiwari-Woodruff S, Kornblum HI: Developmental expression of OSP/claudin-11. J Neurosci Res 60:284–290 (2000).

Byers S, Graham R, Dai HN, Hoxter B: Development of Sertoli cell junctional specializations and the distribution of the tight-junction-associated protein ZO-1 in the mouse testis. Am J Anat 191:35–47 (1991).

Cheng CY, Mruk DD: Cell junction dynamics in the testis: Sertoli-germ cell interactions and male contraceptive development. Physiol Rev 82:825–874 (2002).

Crocker M, Coghill SB, Cortinho R: An unbalanced autosomal translocation (7;9) associated with feminization. Clin Genet 34:70–73 (1988).

Cyr DG, Hermo L, Egenberger N, Mertineit C, Trasler JM, Laird DW: Cellular immunolocalization of occludin during embryonic and postnatal development of the mouse testis and epididymis. Endocrinology 140:3815–3825 (1999).
Debeljuk L, Rao JN, Bartke A: Tachykinins and their possible modulatory role on testicular function: a review. Int J Androl 26:202–210 (2003).
Delva L, Bastie JN, Rochette-Egly C, Kraiba R, Balitrand N, et al: Physical and functional interactions between cellular retinoic acid binding protein II and the retinoic acid-dependent nuclear complex. Mol Cell Biol 19: 7158–7167 (1999).
Dong D, Ruuska SE, Levinthal DJ, Noy N: Distinct roles for cellular retinoic acid-binding proteins I and II in regulating signaling by retinoic acid. J Biol Chem 274:23695–23698 (1999).
Erdman SE, Burtis KC: The *Drosophila* doublesex proteins share a novel zinc finger related DNA binding domain. EMBO J 12:527–535 (1993).
Fairlie WD, Moore AG, Bauskin AR, Russell PK, Zhang HP, Breit SN: MIC-1 is a novel TGF-beta superfamily cytokine associated with macrophage activation. J Leukoc Biol 65:2–5 (1999).
Gow A, Southwood CM, Li JS, Pariali M, Riordan GP, et al: CNS myelin and Sertoli cell tight junction strands are absent in Osp/claudin-11 null mice. Cell 99:649–659 (1999).
Hamer G, Roepers-Gajadien HL, van Duyn-Goedhart A, Gademan IS, Kal HB, et al: DNA double-strand breaks and gamma-H2AX signaling in the testis. Biol Reprod 68: 628–634 (2003).
Hans F, Dimitrov S: Histone H3 phosphorylation and cell division. Oncogene 20:3021–3027 (2001).
Hedger MP: Testicular leukocytes: what are they doing? Rev Reprod 2:38–47 (1997).
Hedger MP: Macrophages and the immune responsiveness of the testis. J Reprod Immunol 57:19–34 (2002).
Heissig B, Hattori K, Dias S, Friedrich M, Ferris B, et al: Recruitment of stem and progenitor cells from the bone marrow niche requires MMP-9 mediated release of kit-ligand. Cell 109:625–637 (2002).
Hodgkin J: The remarkable ubiquity of DM domain factors as regulators of sexual phenotype: ancestry or aptitude? Genes Dev 16: 2322–2326 (2002).
Ion R, Telvi L, Chaussain JL, Barbet JP, Nunes M, et al: Failure of testicular development associated with a rearrangement of 9p24.1 proximal to the *SNF2* gene. Hum Genet 102:151–156 (1998).
Kettlewell JR, Raymond CS, Zarkower D: Temperature-dependent expression of turtle *Dmrt1* prior to sexual differentiation. Genesis 26:174–178 (2000).
Koubova J, Menke DB, Zhou Q, Capel B, Griswold MD, Page DC: Retinoic acid regulates sex-specific timing of meiotic initiation in mice. Proc Natl Acad Sci USA 103:2474–2479 (2006).
Marchand O, Govoroun M, D'Cotta H, McMeel O, Lareyre J, et al: DMRT1 expression during gonadal differentiation and spermatogenesis in the rainbow trout, *Oncorhynchus mykiss*. Biochim Biophys Acta 1493:180–187 (2000).
Matsuda M, Nagahama Y, Shinomiya A, Sato T, Matsuda C, et al: *DMY* is a Y-specific DM-domain gene required for male development in the medaka fish. Nature 417:559–563 (2002).
McGuinness MP, Orth JM: Reinitiation of gonocyte mitosis and movement of gonocytes to the basement membrane in testes of newborn rats in vivo and in vitro. Anat Rec 233: 527–537 (1992).
Meng X, Lindahl M, Hyvonen ME, Parvinen M, de Rooij DG, et al: Regulation of cell fate decision of undifferentiated spermatogonia by GDNF. Science 287:1489–1493 (2000).
Mruk DD, Cheng CY: Sertoli-Sertoli and Sertoli-germ cell interactions and their significance in germ cell movement in the seminiferous epithelium during spermatogenesis. Endocr Rev 25:747–806 (2004).
Nagano R, Tabata S, Nakanishi Y, Ohsako S, Kurohmaru M, Hayashi Y: Reproliferation and relocation of mouse male germ cells (gonocytes) during prespermatogenesis. Anat Rec 258:210–220 (2000).
Nanda I, Shan Z, Schartl M, Burt DW, Koehler M, et al: 300 million years of conserved synteny between chicken Z and human chromosome 9. Nat Genet 21:258–259 (1999).
Nanda I, Kondo M, Hornung U, Asakawa S, Winkler C, et al: A duplicated copy of *DMRT1* in the sex-determining region of the Y chromosome of the medaka, *Oryzias latipes*. Proc Natl Acad Sci USA 99:11778–11783 (2002).
Ogata T, Muroya K, Matsuo N, Hata J, Fukushima Y, Suzuki Y: Impaired male sex development in an infant with molecularly defined partial 9p monosomy: implication for a testis forming gene(s) on 9p. J Med Genet 34:331–334 (1997).
Ogawa T, Ohmura M, Ohbo K: The niche for spermatogonial stem cells in the mammalian testis. Int J Hematol 82:381–388 (2005).
Orth JM, Gunsalus GL, Lamperti AA: Evidence from Sertoli cell-depleted rats indicates that spermatid number in adults depends on numbers of Sertoli cells produced during perinatal development. Endocrinology 122: 787–794 (1988).
Petersen C, Soder O: The Sertoli cell – A hormonal target and 'super' nurse for germ cells that determines testicular size. Horm Res 66: 153–161 (2006).
Raymond CS, Shamu CE, Shen MM, Seifert KJ, Hirsch B, et al: Evidence for evolutionary conservation of sex-determining genes. Nature 391:691–695 (1998).
Raymond CS, Kettlewell JR, Hirsch B, Bardwell VJ, Zarkower D: Expression of *Dmrt1* in the genital ridge of mouse and chicken embryos suggests a role in vertebrate sexual development. Dev Biol 215:208–220 (1999a).
Raymond CS, Parker ED, Kettlewell JR, Brown LG, Page DC, et al: A region of human chromosome 9p required for testis development contains two genes related to known sexual regulators. Hum Mol Genet 8:989–996 (1999b).
Raymond CS, Murphy MW, O'Sullivan MG, Bardwell VJ, Zarkower D: *Dmrt1*, a gene related to worm and fly sexual regulators, is required for mammalian testis differentiation. Genes Dev 14:2587–2595 (2000).
Saitou M, Furuse M, Sasaki H, Schulzke JD, Fromm M, et al: Complex phenotype of mice lacking occludin, a component of tight junction strands. Mol Biol Cell 11:4131–4142 (2000).
Saitou M, Barton SC, Surani MA: A molecular programme for the specification of germ cell fate in mice. Nature 418:293–300 (2002).
Sato M, Kimura T, Kurokawa K, Fujita Y, Abe K, et al: Identification of *PGC7*, a new gene expressed specifically in preimplantation embryos and germ cells. Mech Dev 113:91–94 (2002).
Schneeberger EE, Lynch RD: The tight junction: a multifunctional complex. Am J Physiol Cell Physiol 286:C1213–1228 (2004).
Sharpe RM, McKinnell C, Kivlin C, Fisher JS: Proliferation and functional maturation of Sertoli cells, and their relevance to disorders of testis function in adulthood. Reproduction 125:769–784 (2003).
Shen MM, Hodgkin J: *mab-3*, a gene required for sex-specific yolk protein expression and a male-specific lineage in *C. elegans*. Cell 54: 1019–1031 (1988).
Shima JE, McLean DJ, McCarrey JR, Griswold MD: The murine testicular transcriptome: characterizing gene expression in the testis during the progression of spermatogenesis. Biol Reprod 71:319–330 (2004).
Smith CA, McClive PJ, Western PS, Reed KJ, Sinclair AH: Conservation of a sex-determining gene. Nature 402:601–602 (1999).
Swain A, Zanaria E, Hacker A, Lovell-Badge R, Camerino G: Mouse *Dax1* expression is consistent with a role in sex determination as well as in adrenal and hypothalamus function. Nat Genet 12:404–409 (1996).
Tadokoro Y, Yomogida K, Ohta H, Tohda A, Nishimune Y: Homeostatic regulation of germinal stem cell proliferation by the GDNF/FSH pathway. Mech Dev 113:29–39 (2002).

Tai HH, Ensor CM, Tong M, Zhou H, Yan F: Prostaglandin catabolizing enzymes. Prostaglandins Other Lipid Mediat 68–69:483–493 (2002).

Teranishi M, Shimada Y, Hori T, Nakabayashi O, Kikuchi T, et al: Transcripts of the MHM region on the chicken Z chromosome accumulate as non-coding RNA in the nucleus of female cells adjacent to the *DMRT1* locus. Chromosome Res 9:147–165 (2001).

Vergouwen RP, Jacobs SG, Huiskamp R, Davids JA, de Rooij DG: Proliferative activity of gonocytes, Sertoli cells and interstitial cells during testicular development in mice. J Reprod Fertil 93:233–243 (1991).

Volff JN, Kondo M, Schartl M: Medaka *dmY/dmrt1Y* is not the universal primary sex-determining gene in fish. Trends Genet 19: 196–199 (2003).

Walker WH: Molecular mechanisms controlling Sertoli cell proliferation and differentiation. Endocrinology 144:3719–3721 (2003).

Yamaguchi S, Kimura H, Tada M, Nakatsuji N, Tada T: *Nanog* expression in mouse germ cell development. Gene Expr Patterns 5:639–646 (2005).

Yan HH, Cheng CY: Blood-testis barrier dynamics are regulated by an engagement/disengagement mechanism between tight and adherens junctions via peripheral adaptors. Proc Natl Acad Sci USA 102:11722–11727 (2005).

Yi W, Zarkower D: Similarity of DNA binding and transcriptional regulation by *Caenorhabditis elegans* MAB-3 and *Drosophila melanogaster* DSX suggests conservation of sex determining mechanisms. Development 126:873–881 (1999).

Zarkower D: Establishing sexual dimorphism: conservation amidst diversity? Nat Rev Genet 2:175–185 (2001).

Zhu L, Wilken J, Phillips NB, Narendra U, Chan G, et al: Sexual dimorphism in diverse metazoans is regulated by a novel class of intertwined zinc fingers. Genes Dev 14:1750–1764 (2000).